

Surface morphologies of Pb thin films on Si(111)

This article has been downloaded from IOPscience. Please scroll down to see the full text article.

2007 J. Phys.: Condens. Matter 19 306002

(<http://iopscience.iop.org/0953-8984/19/30/306002>)

View [the table of contents for this issue](#), or go to the [journal homepage](#) for more

Download details:

IP Address: 129.252.86.83

The article was downloaded on 28/05/2010 at 19:52

Please note that [terms and conditions apply](#).

Surface morphologies of Pb thin films on Si(111)

L L Wang¹, X C Ma^{1,3}, P Jiang¹, Y S Fu¹, S H Ji¹, J F Jia² and Q K Xue^{1,2}

¹ Institute of Physics, The Chinese Academy of Sciences, Beijing 100080, People's Republic of China

² Department of Physics, Tsinghua University, Beijing 100084, People's Republic of China

E-mail: xcma@aphy.iphy.ac.cn

Received 13 April 2007, in final form 20 June 2007

Published 11 July 2007

Online at stacks.iop.org/JPhysCM/19/306002

Abstract

Surface morphologies of Pb films prepared on Si(111)- 7×7 substrates are investigated by low temperature scanning tunnelling microscopy. Depending on substrate temperature, coverage and post-deposition annealing temperature and duration, three kinds of morphologies, uniform films, interconnected islands and isolated islands, are formed. In all three cases, preferred heights/thicknesses are observed due to the quantum size effect (QSE) along the surface normal direction. The formation and lateral distribution of either isolated islands or interconnected islands are found to be driven by competition between the boundary formation energy and the long range dipolar repulsive interaction between boundaries. With increasing substrate temperature, the critical thickness for stable films increases, which we attribute to the competition between the long range force induced by the QSE and the elastic force associated with thermal annealing.

(Some figures in this article are in colour only in the electronic version)

1. Introduction

Due to the large lattice mismatch and different bonding nature, epitaxial growth of metal films on semiconductor substrates usually proceeds in the Stranski–Krastanov (SK) or Volmer–Weber (VW) growth mode. An exception is the formation of atomically flat Ag thin films with intriguing thickness-dependent stability on a GaAs(110) surface prepared by a low temperature deposition method [1]. An ‘electronic growth model’ was proposed to explain the novel growth behaviour and the magic stability of the films [2]. According to this model, three competing factors, the quantum size effect (QSE), charge spilling and interface induced Friedel oscillations, determine the critically, magically, or marginally stable, or totally unstable metal films on a semiconductor substrate. Using a similar method, flat films of other metals

³ Author to whom any correspondence should be addressed.

including Al [3] and Pb [4, 5] have been prepared successfully, which also show QSE-facilitated thickness-dependent stability and novel physical properties [6]. In the case of Pb, below the critical thickness of 10 monolayers (ML) [5], islands are formed on a featureless wetting layer (1 ML thick) and their preferred height depends on the substrate temperature and coverage [7–10], and transform into flat-top wedge-shaped islands when warmed up to room temperature [11]. However, there are still some open questions, for example, how does the transition happen in terms of the QSE and thermally induced elastic force and how do the substrate temperature and annealing process influence the morphology?

We report our study on surface morphologies of Pb thin films in the regime of <10 ML on Si(111) prepared and annealed at various temperatures (90 K to room temperature). It is found that when the substrate temperature is 90 K, flat films could be formed at a low coverage of 3.2 ML. With increasing deposition temperature (above 160 K) or coverage (3.2–8.4 ML), surface morphologies evolve into isolated islands or interconnected islands. At 160 K, the uniform Pb film could be obtained only when the coverage increases to 8 ML. Compared to the critical thicknesses of 6 ML at 145 K and 10 ML at room temperature [5], it can be concluded that the critical thickness increases with increasing substrate temperature due to competition between the long range force induced by QSE and the elastic force associated with thermal annealing. In spite of the rich morphologies, while the morphology changes can be essentially understood by the competition between boundary formation energy and the long-range dipole repulsive interactions of boundaries, our observations consistently suggest that QSE along the surface normal direction is always an important factor to be considered for understanding the surface morphology and evolution of this system.

2. Experimental details

The details of the experimental set-up and the procedures for preparation of clean Si(111)- 7×7 surfaces have been described elsewhere [12]. The substrates are n-type Si(111) wafer with a resistivity of $20 \text{ m}\Omega \cdot \text{cm}$. The Si wafer has a miscut angle of 0.2° towards the $[\bar{1}\bar{1}2]$ direction, which produces an average terrace width of about 110 nm separated by monoatomic steps (0.31 nm). Pb(99.999%) was deposited at a flux rate of 0.32 ML min^{-1} . During deposition, the Si(111) substrates were controllably cooled to a certain temperature by the flow rate of liquid nitrogen. Surface morphologies of the samples were characterized *in situ* by a scanning tunnelling microscope (STM). The room temperature annealing was performed by transferring the samples from the STM stage (80 K) to a sample holder at room temperature and leaving them there for a certain time until the required temperature was reached, while for the low temperature annealing experiment a pre-cooled manipulator was used in the MBE chamber. All STM images were acquired at 80 K with a positive bias of 3 V and with a tunnelling current of 100 pA.

3. Results and discussion

3.1. Substrate temperature-dependent morphology

Figures 1(a)–(f) show typical STM images of the as-deposited samples with 4.8 ML Pb at substrate temperatures of 90 K, 170 K, 190 K, 210 K, 240 K and 300 K, respectively. Pb forms (111)-terminated islands/films on Si(111). The statistical area fraction, defined as the fraction of the surface area of all islands to the total surface area, and the island density, defined as the number of islands per μm^2 , are shown in figure 1(g), while the island height distribution is given in figure 1(h). The island heights were measured above the wetting layer, while the layer

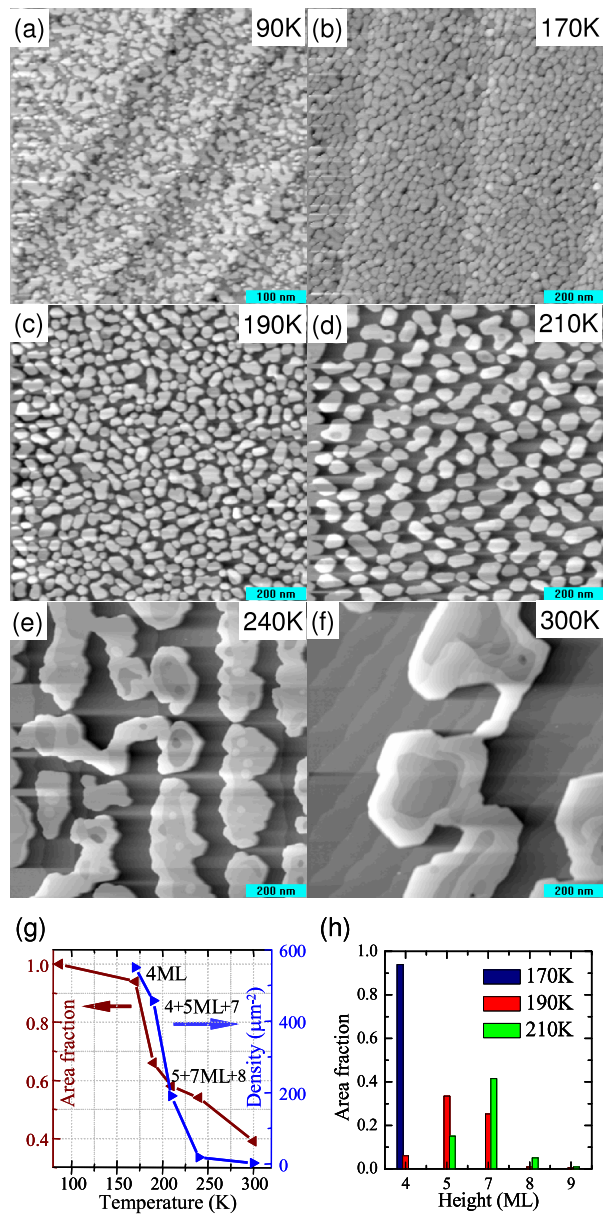


Figure 1. STM images obtained after 4.8 ML Pb was deposited on Si(111) at different temperatures: (a) 90 K (500 nm × 500 nm), (b) 170 K (1000 nm × 1000 nm), (c) 190 K (1000 nm × 1000 nm), (d) 210 K (1000 nm × 1000 nm), (e) 240 K (1000 nm × 1000 nm) and (f) room temperature (1000 nm × 1000 nm). (g) The statistical area fraction and island density statistics and (h) the height distribution show that with increasing substrate temperature, island density decreases and height increases in the bi-layer. The numbers labelled in (g) indicate the preferred heights of Pb islands, while the central numbers with bigger font size and suffixed ML indicate the most preferred ones.

counting of the films includes the 1 ML thick wetting layer. At a substrate temperature of 90 K, the film is almost continuous, while at 170 K uniform small islands 4 ML high are formed. Isolated flat-topped islands are observed when the substrate temperature increases to 190 and

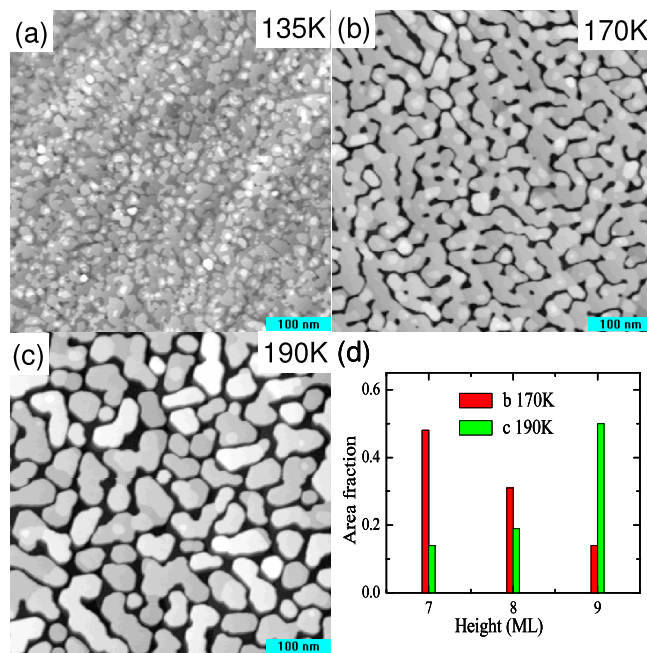


Figure 2. STM images ($500 \text{ nm} \times 500 \text{ nm}$) obtained after 8.4 ML Pb was deposited at different substrate temperatures: (a) 135 K, (b) 170 K and (c) 190 K. (d) The corresponding height distribution shows that the islands grow in height and the heights are preferential for odd-numbered layers.

210 K. At 190 K, all islands are in the same terraces with three preferred heights of 5, 7 and 4 ML in order of preference. At 210 K, the preferred heights change to 7, 5 and 9 ML, and a few flat-topped islands crossing the Si steps appear. With increasing substrate temperature (240 K and room temperature), islands crossing two and more Si steps are observed. The preferred heights of 4, 5, 7 and 9 ML have been shown to be related to the interplay between the QSE and the discrete nature of the lattice spacing [2, 4, 9, 10]. With increasing temperature, the diffusion of Pb atoms increases so that the island density decreases and the height increases correspondingly. Therefore, 210 K is the temperature at which diffusion between adjacent terraces takes place.

Figures 2(a)–(c) show typical STM images of the as-deposited samples with 8.4 ML Pb at 135, 170 and 190 K. Complete films could be obtained when the substrate temperature was below 135 K. At 170 and 190 K, interconnected islands and isolated islands are formed, respectively. The corresponding height histograms of figures 2(b) and (c) are shown in figure 2(d), which indicates that the most preferred heights are 7 and 9 ML. Islands of 8 ML appear only when the islands cross Si steps. The similarly increasing preferred height and morphology change with increasing substrate temperatures can be understood by enhanced kinetics. Different from the isolated islands formed for a 4.8 ML coverage at the same temperature (170 K), interconnected islands are formed here. Another difference is that many islands crossing Si steps are observed at 190 K, while the wedge-shaped islands only appear occasionally at 210 K in the case of 4.8 ML.

3.2. Room temperature morphology evolution

To study thermally induced morphology evolution, the as-deposited Pb films at 90 K (3.2 and 4.8 ML) were annealed at room temperature. Figure 3(a) shows a typical STM image of a

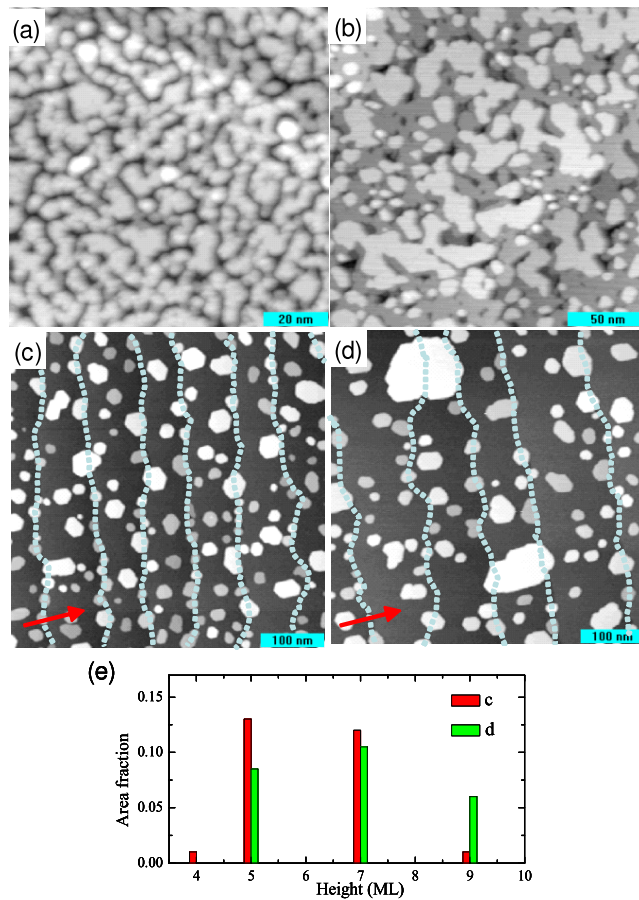


Figure 3. STM images obtained after 3.2 ML Pb was deposited on Si(111) at 90 K (a) ($100\text{ nm} \times 100\text{ nm}$), and annealed at room temperature for 8 min (b) ($200\text{ nm} \times 200\text{ nm}$), an additional 24 min (c) ($500\text{ nm} \times 500\text{ nm}$) and a further 30 min (d) ($500\text{ nm} \times 500\text{ nm}$). In (c) and (d), the dotted lines indicate the steps on the Si(111) surfaces, and the arrows indicate the direction of atomic steps running upwards. (e) The corresponding height distribution shows that the heights of isolated islands cover a wide range.

3.2 ML Pb film prepared at 90 K. The surface morphology is nearly the same as that of the 4.8 ML film (figure 1(a)), due to limited atomic diffusion at low temperature. After annealing for 8 min at room temperature, the surface becomes smoother, but some voids appear down to the wetting layer (figure 3(b)). Dramatic morphological change into isolated islands is observed after the sample is annealed for an additional 24 and 54 min (figures 3(c) and (d)). As shown in figure 3(c), about half of the islands are located along the upper terraces of the Si(111) substrate (the steps are indicated by dotted lines). In figure 3(d), we can see that both the island density and the number of islands along substrate steps decrease, and larger islands crossing Si steps are formed. All these islands show a very clear height preference depending on the annealing time. As seen from the height histogram (figure 3(e)), the preferred heights are 4, 5 and 7 ML for the islands in figure 3(c), and 5, 7 and 9 ML for those in figure 3(d).

If the 4.8 ML sample (figure 1(a)) was treated using the same annealing process, the surface looks basically similar to that of the 3.2 ML samples (figure 3(b)), except for the island

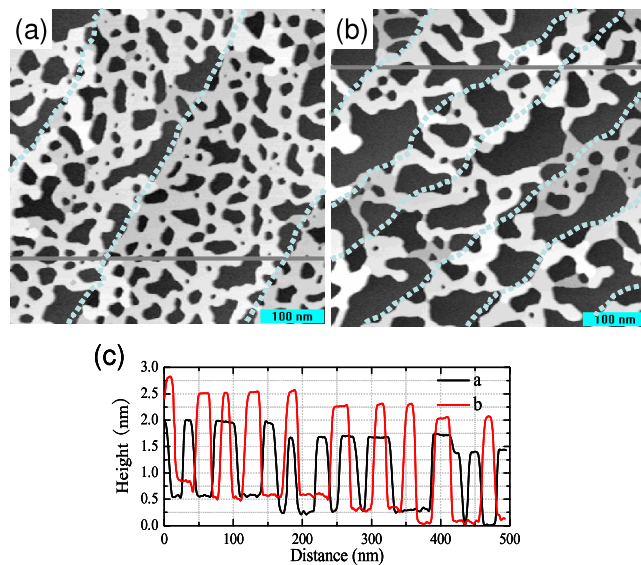


Figure 4. STM images ($500 \text{ nm} \times 500 \text{ nm}$) obtained after 4.8 ML Pb was deposited at 90 K and annealed for 8 min and an additional 24 min (a), and a further 30 min (b). (c) The corresponding line profile shows that the interconnected islands in (a) ((b)) are exclusively 5 ML (7 ML) high. The dotted lines indicate the steps on the Si(111) surfaces.

height. However, after the additional 24 min (figure 4(a)) and 54 min (figure 4(b)) annealing, interconnected islands are formed. A similar step-crossing effect is observed clearly, especially in figure 4(a), as the void density along the Si(111) steps is much lower than that on the terraces. Figure 4(c) shows the line profiles of those indicated by the black lines in figures 4(a) and (b). The heights of the interconnected islands are exclusively 5 ML in figure 4(a) and 7 ML in figure 4(b).

During annealing, Pb atoms move upward to reduce the interface strain associated with the large lattice mismatch (34.7%) between Si and Pb, which cannot happen at low temperature where the necessary kinetics is frozen. The vertical motion can be identified even after the 8 min annealing, as some voids down to the wetting layer have already appeared (figure 3(b)). In the further annealing process, the thicknesses of films/islands increase at the expense of void formation and growth, as required by mass conservation. Films evolve into isolated islands in the case of 3.2 ML and interconnected islands in the case of 4.8 ML, with an area fraction of 27% (figure 3(c)) and 66% (figure 4(a)), respectively. The formation of two patterns is easy to understand since 3.2 ML is less than 3.5 ML, the lowest coverage needed for growth of the 1.5 ML high wetting layer and the 4 ML (the lowest magic height) islands covering half of the surface, whereas 4.8 ML satisfies this condition. The difference in morphology is still obvious even after additional annealing for 54 min by comparing the area fraction of 25% (figure 3(d)) and 48% (figure 4(b)), which will be discussed below.

Once voids are formed, the surface exhibits two domain structures, the disordered wetting layer and the (111)-oriented Pb layer. It is well known that it costs energy to create a domain boundary, so small domains are thermodynamically unstable and will coarsen into large domains during annealing. However, there is a long range dipolar repulsive interaction between domain boundaries arising from the difference in surface stress between the Pb islands and the wetting layer, which favours small domains [13, 14]. Consequently, besides

the magic height determined by QSE along the normal direction, in the lateral direction the competition between the boundary formation energy and the long range dipolar repulsive interaction between boundaries leads to different patterns, i.e. the isolated islands at 3.2 ML and the interconnected islands at 4.8 ML.

With enhanced atom diffusion upon further annealing, both isolated and interconnected islands grow vertically as driven by the interface strain. Accordingly, the boundary free energy increases, but the dipolar repulsive interaction decreases with increasing distance between boundaries. That is, with increasing annealing time, the boundary formation energy gradually overrides the dipolar repulsive interaction, so that the sizes of isolated and interconnected islands increase (compare figures 3(c) and (d), and 4(a) and (b)). When the annealing time is long enough (4 h), both isolated islands and interconnected islands eventually evolve into thermally stable flat-topped wedge-shaped islands driven by surface energy minimization [11].

Another interesting observation is the different preferred heights for the isolated and interconnected islands. As mentioned above, 4, 5, 7 and 9 ML are preferred heights by QSE; usually three of them are present for the isolated islands. On the other hand, the interconnected islands in figure 4(a) are exclusively 5 ML (7 ML for figure 4(b)) high. The 3.2 ML films evolve into isolated islands, and some islands grow larger and higher at the expense of some smaller ones with annealing. The randomization in this course determines the widely ranging heights. At the same time, the more the wetting layer is exposed, the longer the boundary is, and the larger the probability of upward diffusion is. That is the reason why higher islands appear earlier on the 3.2 ML sample. For example, 9 ML islands appear even after the additional 24 min annealing. In the case of 4.8 ML, atom diffusion is limited within the terrace, as revealed by the fact that the area fractions on all the terraces take the same values of 66% in figure 4(a) and 48% in figure 4(b). The singular preferred height of the interconnected islands implies that the energy gain induced by QSE can compensate for the free energy loss associated with formation of Pb steps.

3.3. Critical temperature for stable 8 ML films

According to our previous studies [5], the critical thickness for the formation of uniform films is 6 ML at 145 K, and it is 10 ML at room temperature. No uniform films of 7 and 9 ML have been observed because of the interplay between QSE and elastic interaction [5, 8, 15, 16]. In order to identify the critical temperature for stable 8 ML film, annealing experiments were performed for the 8.4 ML samples prepared at 135 K (figure 2(a)).

Figures 5(a) and (b) show typical STM images after the sample is annealed at room temperature. Voids appear after annealing (figure 5(a)), and interconnected islands with a singular magic height of 9 ML are formed after an additional 20 min annealing (figure 5(b)). The characteristic of singular magic height, similar to that in room temperature annealing of the 4.8 ML film, indicates confined diffusion within terraces. In contrast, when the sample is annealed at 160 K for 50 min, a uniform film is formed (figure 5(c)). After an additional 50 min annealing at 190 K, voids with a depth of 9 ML are formed (figure 5(d)), indicating that the critical thickness for formation of stable Pb films at 160 K is 8 ML. It is worth mentioning that most voids formed after annealing are hexagonal due to the three-fold symmetry and locate near Si(111) steps, similar to the behaviour of isolated islands in figures 3(c) and (d). The result of the critical thickness of 8 ML at 160 K is consistent with the previous observation of 6 ML at 145 K and 10 ML at room temperature [5], and can be understood qualitatively as follows. The critical thickness is determined by the balance between the long range force induced by QSE and the elastic force induced by the lattice mismatch [16]. When the temperature is increased, the lattice mismatch increases thermally, and a new balance needs to be re-established by energy

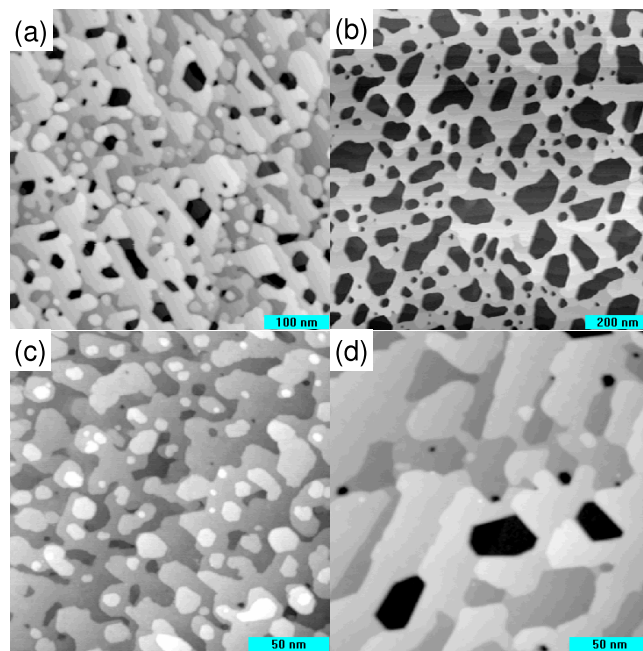


Figure 5. STM images after an 8.4 ML Pb film prepared at 135 K was annealed at room temperature for 6 min (a) ($500 \text{ nm} \times 500 \text{ nm}$) and an additional 20 min (b) ($1000 \text{ nm} \times 1000 \text{ nm}$); or annealed at 160 K for 50 min (c) ($200 \text{ nm} \times 200 \text{ nm}$) and at 190 K for an additional 50 min (d) ($200 \text{ nm} \times 200 \text{ nm}$).

gain from QSE at increasing thickness. On the other hand, once uniform films have formed at low temperatures, formation of voids becomes more difficult for thicker films, since boundary formation is thermodynamically unfavourable and costs more energy with increasing thickness.

4. Conclusion

The morphologies of Pb films on Si(111) prepared and annealed at various temperatures have been studied by STM. The temperature and coverage dependent morphology patterns are found to be controlled by two competing mechanisms. One is competition between the long range force induced by QSE and the elastic force along the normal direction, which determines the critical thickness for stable films at a given temperature. The other is the lateral competition between boundary formation and the long range dipolar repulsive interaction between boundaries, which leads to the formation of coverage-dependent patterns during annealing.

Acknowledgments

This work was supported by the National Science Foundation and Ministry of Science and Technology of China.

References

- [1] Smith A R, Chao K-J, Niu Q and Shih C-K 1996 *Science* **273** 226
- [2] Zhang Z, Niu Q and Shih C-K 1998 *Phys. Rev. Lett.* **80** 5381
- [3] Liu H, Zhang Y F, Wang D Y, Pan M H, Jia J F and Xue Q K 2004 *Surf. Sci.* **571** 5

- [4] Upton M H, Wei C M, Chou M Y, Miller T and Chiang T-C 2004 *Phys. Rev. Lett.* **93** 26802
Czoschke P, Hong H, Basile L and Chiang T-C 2004 *Phys. Rev. Lett.* **93** 36103
- [5] Zhang Y F, Tang Z, Han T Z, Jia J F and Xue Q K 2005 *Surf. Sci.* **596** L331
- [6] Guo Y, Zhang Y F, Bao X Y, Han T Z, Tang Z, Zhang L X, Zhu W G, Wang E G, Niu Q, Qiu Z Q, Jia J F, Zhao Z X and Xue Q K 2004 *Science* **306** 1915
- [7] Hupalo M, Kremmer S, Yeh V, Bautista L B, Abram E and Tringides M C 2001 *Surf. Sci.* **493** 526
Budde K, Abram E, Yeh V and Tringides M C 2000 *Phys. Rev. B* **61** 10602
Yeh V, Bautista L B, Wang C Z, Ho K M and Tringides M C 2000 *Phys. Rev. Lett.* **85** 5158
- [8] Su W B, Chang S H, Jian W B, Chang C S, Chen L J and Tsong T T 2001 *Phys. Rev. Lett.* **86** 5116
Chang S H, Su W B, Jian W B, Chang C S, Chen L J and Tsong T T 2002 *Phys. Rev. B* **65** 245401
- [9] Hong H, Wei C-M, Chou M Y, Wu Z, Basile L, Chen H, Holt M and Chiang T-C 2003 *Phys. Rev. Lett.* **90** 76104
- [10] Özer M M, Jia Y, Wu B, Zhang Z and Weiering H H 2005 *Phys. Rev. B* **72** 113409
- [11] Altfeder I B, Matveev K A and Chen D M 1997 *Phys. Rev. Lett.* **78** 2815
Li S-C, Ma X C, Jia J F, Zhang Y F, Chen D M, Niu Q, Liu F, Weiss Paul S and Xue Q K 2006 *Phys. Rev. B* **74** 075410
Li S-C, Jia J F, Ma X C, Xue Q K, Han Y and Liu F 2006 *Appl. Phys. Lett.* **89** 123111
- [12] Wang L L, Ma X C, Jiang P, Fu Y S, Ji S H, Jia J F and Xue Q K 2006 *Phys. Rev. B* **74** 073404
- [13] Plass R, Last J A, Bartelt N C and Kellogg G L 2001 *Nature* **412** 875
- [14] Plass R, Bartelt N C and Kellogg G L 2002 *J. Phys.: Condens. Matter* **14** 4227
van Gastel R, Plass R, Bartelt N C and Kellogg G L 2003 *Phys. Rev. Lett.* **91** 55503
- [15] Zhang Y F, Jia J F, Han T Z, Tang Z, Shen Q T, Guo Y, Qiu Z Q and Xue Q K 2005 *Phys. Rev. Lett.* **95** 96802
- [16] Suo Z and Zhang Z 1998 *Phys. Rev. B* **58** 5116